340

Reprinted from the Proceedings of the Symposium on
WATERSHED MANAGEMENT '80
ASCE/Boise, ID/July 21–23, 1980

MODELING CHANNEL PROCESSES WITH CHANGING LAND USE

Leonard J. Lane, AM, ASCE, and George R. Foster[1]

ABSTRACT

Procedures are developed to predict channel morphology for small streams and to relate channel morphology to sediment yield. Sensitivity analysis shows the response or adjustment of stream channels due to changes in discharge and channel characteristics resulting from changing land use. The procedure provides a basis, from hydraulics of open channel flow and a simple erosion equation, to quantitatively evaluate the response of stream channels to changes in discharge, soil properties, and topography. The quantitative method is an improvement over qualitative procedures based on empirical regression equations.

INTRODUCTION

To assess the response of stream channels to changing land use, it is necessary to express the relations between channel morphology and sediment yield. The importance of channel processes in determining sediment yield is especially critical in channel systems that are developing or eroding.

Relationships between hydrologic and hydraulic factors and geometry of the channel are referred to as hydraulic geometry (11). Numerous investigators have confirmed generalized hydraulic geometry relations, for example, Leopold, Wolman, and Miller (13), Chapter 7. However, in spite of the extensive body of literature dealing with hydraulic geometry, there is a need for equations that express the hydraulic geometry relations in terms of channel properties and hydraulic processes. Expressions that describe the controlling processes can facilitate the extension of prediction equations to ungaged streams.

The purpose of this study was to examine relations between channel morphology and sediment yield, and to develop expressions for the hydraulic geometry equations that incorporate (a) channel properties, (b) a simplified erosion equation, and (c) hydraulic properties of steady flow in small stream channels. Although the upland or overland and channel processes are interrelated and complex, we sought to isolate and analyze the channel component independent of the overland processes. We assumed quasi-steady state relationships of normal flow and development

[1]The authors are hydrologist, U.S. Department of Argicultùre, Science and Education Administration, Agricultural Research (USDA-SEA-AR), Southwest Rangeland Watershed Research Center, Tucson, Arizona 85705, and hydraulic engineer, U.S. Department of Agriculture, Science and Education Administration, Agricultural Research (USDA-SEA-AR), Department of Agricultural Engineering, Purdue University, West Lafayette, Indiana 47907.

of a final eroded channel width. We also assumed that detachment rather than sediment deposition controlled sediment yield from small channels. Finally, we emphasized small and very small channels such as: (a) erosional channels that develop in areas where flow is concentrated such as stream headwaters, terrace channels, etc., (b) small channels that are permanent features of the landscape and are normally "tilled over" during cultivation, and (c) temporary channels that develop when field rows or terraces overtop, such as very small gullies or rill systems. The equilibrium or quasi-steady state relationships apply to concentrated flow in upland areas, and the derived relationships are related to empirical results from hydraulic geometry investigations. The results and validity of extension of the results to larger channels are discussed in a later section of the paper.

BACKGROUND

Hydraulic geometry consists of a set of equations representing relationships between width, depth, and velocity of flow, and a characteristic discharge in open channel flow (11). The usual form of these equations is as follows:

channel width is $$w = aQ^b , \tag{1}$$

average depth of flow is $$d = cQ^f , \tag{2}$$

average velocity is $$v = kQ^m , \tag{3}$$

where in English units: Q = discharge rate (cfs),
w = average width of flow (ft),
d = average depth of flow (ft), and
v = average velocity (ft/sec).

The continuity equation $$Q = Av = wdv \tag{4}$$

requires that $$ack = 1.0 \tag{5}$$

and $$b + f + m = 1.0. \tag{6}$$

If S is the friction slope (equal to the bed slope for normal flow) and n is the Manning hydraulic resistance parameter, then these parameters are assumed to be related to the discharge as

$$S = tQ^z \tag{7}$$

$$n = rQ^y . \tag{8}$$

Equations 1-8 are the hydraulic geometry equations with a, c, k, t, and r as coefficients and b, f, m, z, and y as exponents.

For wide, nearly rectangular channels, the depth of flow is approximately equal to the hydraulic radius so that the Manning velocity equation is

$$v = \frac{1.49}{n} S^{1/2} d^{2/3} . \tag{9}$$

Equating this velocity to the velocity from Eq. 3 results in the following equations:

$$k = 1.49\ r^{-1} t^{1/2} c^{2/3} \tag{10}$$

and

$$m = -y + 1/2\ z + 2/3\ f \tag{11}$$

as additional constraints.

Relations At a Station and Downstream:

Hydraulic geometry at a station refers to the equations for discharges of different frequencies at a particular cross section. Downstream hydraulic geometry refers to the equations at downstream locations for discharge of the same frequency (constant at a given cross section but increasing in the downstream direction). Although the same basic equations apply at a station and in the downstream direction, the coefficients and exponents may be different (8).

Most streams tend to be concave, resulting in a decrease in slope in the downstream direction (6). Manning's n also has been observed to vary with the depth of flow, and thus with the discharge (16). The majority of empirical evidence suggests that z and y in Eqs. 7 and 8 are usually negative. For measurements at a station, z is usually near zero and y is somewhat less than zero. For measurements downstream, z is usually negative and on the order of 2 to 5 times y.

Comparison of the hydraulic geometry at a station with that downstream can be made by combining Eqs. 4 and 9 and examining the resulting exponents. For example, the exponent m in Eq. 3 is given by Eq. 11. Since m involves -y and +1/2 z, lower values of m are expected for the downstream direction than at a station. Values of z and y for a variety of conditions from a number of sources are summarized in Table 1. Coefficients for hydraulic geometry equations for two downstream situations and one situation at a station are summarized in Table 2.

The data in Table 2 represent variation in the coefficients associated with assumed values of the exponents. Additional values of the hydraulic geometry exponents are presented in Leopold, Wolman, and Miller (13), Chapter 7, pp. 244 and 271.

Hydraulic Geometry for Nonerodible Channels:

In triangular channels (triangular cross-section) it is possible to solve for d, w, and v as explicit functions of the discharge in normal flow. In a triangular cross-section, if s is the side slope of the channel banks, then the geometrical relationships are as follows. The cross-sectional area is

$$A = \frac{1}{s} d^2 \tag{12}$$

the top width is

$$w = \frac{2}{s} d \tag{13}$$

and the hydraulic radius R is

$$R = \frac{1}{2} \left(\frac{1}{1+s^2}\right)^{1/2} d = \frac{1}{2c} d\ . \tag{14}$$

TABLE 1.—ASSUMPTIONS ON SLOPE (z) AND RESISTANCE (y) EXPONENTS FOR VARIOUS HYDRAULIC CONDITIONS

Condition	Slope exponent z $S = tQ^z$	Resistance exponent y $n = rQ^y$	Source
Rivers, in downstream direction.	-0.73	-0.22	Theory; Leopold, Wolman, and Miller (13), p. 271
	-0.75	-0.15	Data; Ibid
	-0.49[1]	--	Data; Leopold and Maddock (11), p. 26
	-1.07	-0.28	Data; Wolman (20), pp. 23, 26
	-0.95[2]	-0.30[2]	Data; Leopold, Wolman, and Miller (13), p. 244
	-0.23[3]	-0.14[3]	Data; Ibid, p. 257
	-0.38	0.0	Data; Ibid
Rivers, at a station, cohesive.	0.0	- .035	Theory; Ibid, p. 271
	0.0[4]	-0.16[4]	Experimental rill study; Foster and Lane (2)
Rivers, at a station, noncohesive.	---	- .04	Theory; Leopold, Wolman, and Miller (13), p. 271
Rivers, at a station.	+0.05	- .20	Data; Wolman (20), pp. 23, 26

[1] Average value for midwestern U.S.
[2] Ephemeral streams in semiarid U.S.
[3] Ephemeral streams in New Mexico.
[4] Experimental data for rills developing in cohesive soil.

Now, since

$$Q = Av = \frac{1.49}{n} S^{1/2} R^{2/3} A \qquad (15)$$

Equation 15 can be solved for the depth d, and then the other hydraulic geometry equations follow from the above relationships. The depth of flow is

$$d = \left(\frac{s}{1.49}\right)^{3/8} (2c)^{1/4} S^{-3/16} n^{3/8} Q^{3/8} \qquad (16)$$

which from Eqs. 7 and 8 becomes

$$d = t^{-3/16} r^{3/8}\left(\frac{s}{1.49}\right)^{3/8} (2c)^{1/4} Q^{[-3z/16 + 3(y+1)/8]}. \qquad (17)$$

From Eq. 17 and Eq. 13, the width is

$$w = \frac{2}{s} t^{-3/16} r^{3/8} \left(\frac{s}{1.49}\right)^{3/8} (2c)^{1/4} Q^{[-3z/16 + 3(y+1)/8]}. \qquad (18)$$

TABLE 2.—COEFFICIENTS IN SELECTED HYDRAULIC GEOMETRY EQUATIONS AND CHARACTERISTICS OF SEDIMENT-TYPE CHANNELS

Variable	Coefficient in Hydraulic Geometry Equation		Character of channel
	a[1]	c	Data from Osterkamp (14)
Width	2.77	---	Silt-clay of bed material: 70-100%
$w = aQ^b$	3.73	---	Silt-clay of bed material: 30-69%
Depth			
$d = cQ^f$	4.15	---	Silt-clay of bed material: 7-29%
	5.87	---	Silt-clay of bed material: <7% and Silt-clay of bank material: ≥ 50%
	6.74	---	Silt-clay of bed material: <7% and Silt-clay of bank material: <50%
	a[1]	c[2]	Data from Henderson (5)
	1.53	.41	Sand bed and cohesive banks with heavy sediment load
	1.58	.28	Coarse noncohesive material
	1.98	.45	Cohesive bed and banks
	2.34	.53	Sand bed and cohesive banks
	3.15	.63	Sand bed and banks
	a[3]	c	Data from Foster and Lane (2)
	2.64	.09	Rills developing in cohesive soil

[1] Osterkamp and Henderson assumed b = 1/2 for downstream relations.
[2] Henderson assumed f = 0.36 for downstream relations.
[3] Foster and Lane found b = .48 and f = 0.21 for relations at a station.

The velocity is v = Q/A which is

$$v = st^{3/8}\, r^{-3/4} \left(\frac{s}{1.49}\right)^{-3/4} (2c)^{-1/2}\, Q^{[1+3z/8 - 3(y+1)/4]}. \quad (19)$$

Therefore, the hydraulic geometry exponents are

$$b = f = -3z/16 + 3(y+1)/8 \quad (20)$$

and

$$m = 1 + 3z/8 - 3(y+1)/4. \quad (21)$$

In a uniform, nonerodible triangular channel, if all the flow is within the channel, the only widening with increasing discharge is due to increases in depth. Under these conditions, Eqs. 20 and 21 can be used to compare exponents at a station and downstream. If we assume z = 0 at a station, and z < 0 downstream, then

$$b_d = -3z/16 + b_s, \quad (22)$$

$$f_d = -3z/16 + f_s, \tag{23}$$

and

$$m_d = 3z/8 + m_s \tag{24}$$

where the subscript d refers to relations downstream and the subscript s refers to relations at a station. For negative values of the slope exponent z, the values of b and f are always larger downstream than at a station, and the value of m is always less downstream than at a station.

For a wide, nonerodible rectangular channel, if the depth is assumed equal to the hydraulic radius, the hydraulic geometry equations are:

$$w = w_o = \text{constant} \tag{25}$$

$$d = \left(\frac{1}{1.49w}\right)^{3/5} t^{-3/10}\, r^{3/5}\, Q^{[-3z/10 + 3(y+1)/5]} \tag{26}$$

and

$$v = \frac{(1.49)^{3/5}}{w^{2.5}}\, t^{3/10}\, r^{-3/5}\, Q^{[1 + 3z/10 - 3(y+1)/5]}. \tag{27}$$

From these equations

$$b = 0, \tag{28}$$

$$f = -3z/10 + 3(y+1)/5, \tag{29}$$

and

$$m = 1 + 3z/10 - 3(y+1)/5. \tag{30}$$

Corresponding to Eqs. 22-24, the relations between values of exponents downstream and at a station are

$$b_d = b_s = 0, \tag{31}$$

$$f_d = -3z/10 + f_s, \tag{32}$$

and

$$m_d = 3z/10 + m_s. \tag{33}$$

Thus, for a nonerodible rectangular channel and negative values of the slope exponent z, the exponent b is the same downstream as at a station; the exponent f is larger downstream than at a station, and the exponent m downstream is less than at a station.

Values of hydraulic geometry exponents for nonerodible triangular and rectangular channels and for typical slope and resistance exponents are summarized in Table 3.

Examination of the data shown in Table 3 allowed us to consider the effects of cross-sectional shape, decrease in resistance due to increasing depth, and decrease in resistance and slope upon the hydraulic geometry exponents.

Effects of Cross-sectional Geometry. Row 1 of Table 3 (at a station, z = 0, y = 0) represents the influence of cross-sectional shape on hydraulic geometry. As expected, the depth and velocity increase more rapidly in a rectangular channel than in a triangular channel, while the width remains constant in a rectangular channel.

TABLE 3.—VALUES OF HYDRAULIC GEOMETRY EXPONENTS; $w = aQ^b$, $d = cQ^f$, AND $v = kQ^m$ FOR NONERODIBLE TRIANGULAR AND RECTANGULAR CROSS-SECTIONS

Condition	Triangular Cross Section			Rectangular Cross Section		
	Width b	Depth f	Velocity m	Width b	Depth f	Velocity m
At a station $z = 0$ $y = 0$	0.3750	0.3750	0.2500	0.0	0.6000	0.4000
At a station $z = 0$ $y = -0.15$	.3188	.3188	.3625	0.0	.5100	.4900
Downstream $z = -0.75$ $y = -0.15$	.4594	.4594	.0813	0.0	.7350	.2650

Effects of Decreasing Resistance. Rows 1 and 2 of Table 3 represent the influence of decreasing resistance with increasing discharge. With decreasing hydraulic resistance, the width and depth increase at a slower rate while the velocity increases at a faster rate.

Effects of Decreasing Slope and Resistance. Row 3 of Table 3 represents the downstream influence of decreasing slope and resistance. Again, width and depth increase at a faster rate with increasing discharge, while velocity increases at a slower rate.

Since a trapezoidal cross-section is a composite of triangular and rectangular cross-sections, the hydraulic geometry exponents should be between those of triangular and rectangular cross-sections.

Extension to Erodible Channels:

As erosion widens an erodible channel with increasing discharge, the width should increase faster and the depth and velocity should increase more slowly than in nonerodible channels. Table 4 shows average values of hydraulic geometry exponents for streams in the midwestern United States (13) in comparison with the derived values for a nonerodible rectangular channel.

We now examine a simplified model for the case of an erodible channel.

DEVELOPMENT OF A SIMPLIFIED MODEL

For rectangular channels and complex shear stress distributions, it is not possible to explicitly solve for the depth or width of flow (as in Eqs. 26 and 27). Therefore, we developed an implicit solution for the final eroded width.

Implicit Solution:

A simplified relationship among channel features, discharge, and equilibrium or final eroded channel width was derived and tested. Experiments to collect data on sediment yield with time were done only for

TABLE 4.—COMPARISON OF OBSERVED HYDRAULIC GEOMETRY EXPONENTS FOR MIDWESTERN UNITED STATES STREAMS WITH DERIVED VALUES FOR A NONERODIBLE RECTANGULAR CHANNEL

Condition	Midwestern Streams			Nonerodible Rectangular Cross-Section		
	Width b	Depth f	Velocity m	Width b	Depth f	Velocity m
At a station	0.26	0.40	0.34	0.0	0.51[1]	0.49
Downstream	.50	.40	.10	0.0	.74[2]	.26

[1]Assuming z = 0.0 and y = -0.15
[2]Assuming z = -0.75 and y = -0.15

rill erosion studies, but a large number of quasi-equilibrium widths corresponding to the principal channel-forming discharge were obtained from the literature.

The model simulates channel development in homogeneous erodible material and in material with an erosion resistant or nonerodible boundary. Input to the model consists of a flow rate, a channel slope, hydraulic resistance parameter, soil erodibility factor, a critical shear stress, and the shear stress distribution around the channel cross-section.

When a nonerodible boundary is present and the channel erodes down to this boundary, the procedure is to find the normalized distance from the water surface down to the point where the shear stress equals the critical shear stress. When this distance x is equal to the depth of flow, then the shear stress on the channel bank will be less than the critical shear stress, and since the channel bottom is nonerodible, the channel will stop eroding and not widen. This is the final eroded width W_f. This final eroded width is

$$W_f = \left[\frac{nQ}{1.49\, S^{1/2}}\right]^{3/8} \left[\frac{1 - 2\, x_*}{x_*^{5/8}}\right]^{3/8} \tag{34}$$

where x_* is the distance x normalized by the length of the wetted perimeter. Values of x_* were computed numerically for a rectangular cross-section (2).

Once the nonerodible boundary is reached, but before the final eroded width is reached, erosion rates decrease exponentially with time as

$$E(t) = E_o\, d_{soil}\, \rho_s \exp(-t_*) \tag{35}$$

where E(t) is erosion rate with time, d_{soil} is the depth of the soil, ρ_s is the specific weight of the soil, and t_* is the normalized time. This normalized time t_* is computed from

$$t_* = tE_o/(W_f - W_{ac}) \tag{36}$$

where t is time since the erodible boundary was reached, E_o is the initial rate that the channel widens, W_f is the final eroded width from Eq. 34, and W_{ac} is the equilibrium width of the rectangular channel before the nonerodible boundary is reached.

Equations 34-36 provide a means of computing widths and associated erosion rates for eroding channels in homogeneous soil under circumstances where a nonerodible boundary is present.

The procedures described above were applied to data from an experimental rill erosion study where channel (rill) cross-sections, flow variables, and sediment yield were measured under controlled conditions. A nonerodible boundary was present below the soil surface.

Comparisons of observed and computed sediment yields with time showed a good fit using the simple model. Total sediment yields over the seven replicated runs produced a relation between observed sediment yield Q_s, and computed sediment yield $\widehat{Q}_s$ as

$$\widehat{Q}_s = -11.0 + 0.93\ Q_s \tag{37}$$

with an $R^2 = 0.97$. Therefore, we believe the model reproduced observed sediment yields within measurement accuracy.

In the rill erosion studies, discharge, slope, and channel geometry were measured, which allowed direct estimation of Manning's n. However, to apply the model to selected discharge-width data from the literature, we had to estimate the n values (1). Given these estimates, the model was used to compute final widths, W_f, and these were compared with measured values. Osterkamp (14) selected a number of streams in the mountains and high plains of the United States and related channel width to a characteristic discharge. Observed and computed data for Osterkamp's 32 streams and the rills are shown in Fig. 1. Widths and discharges were then related by regression of the form

$$w = a\ Q^b \tag{38}$$

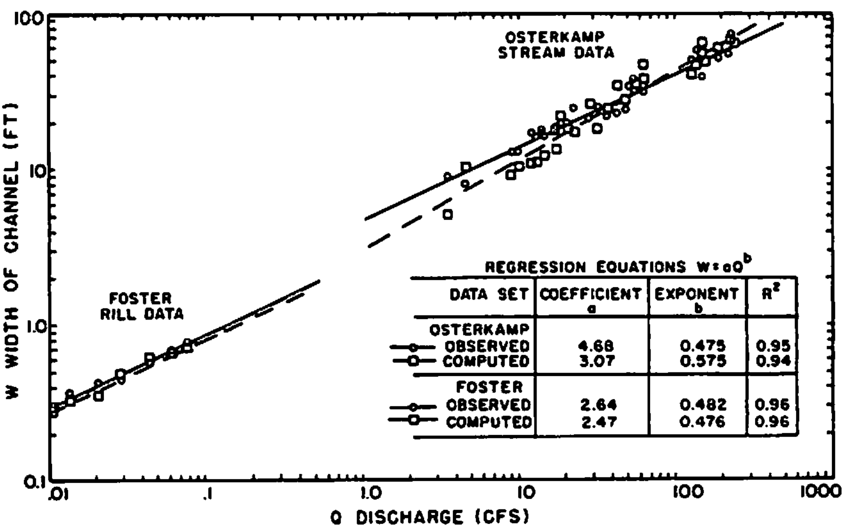

FIG. 1.—RELATION BETWEEN CHANNEL DISCHARGE AND WIDTH FOR NATURAL STREAMS AND EXPERIMENTAL RILL SYSTEMS

following the procedure outlined by Leopold and Miller (12). These regression results for the observed and computed channel widths are shown in Fig. 1. For natural streams, the exponent b was larger for the computed widths than for the observed data. In these wide, natural streams, the distribution of shear stress around the channel cross-section may be more uniform and nearer to the average shear stress over the wetted perimeter than was assumed. Nonetheless, as shown in Fig. 1, the model is a reasonable approximation of the observed width-discharge relationship.

These analytic procedures relating hydraulic variables, soil properties, and channel geometry to sediment yield with time in a developing channel system tend to agree with empirical observations, suggesting an exponential decay in sediment yield with time (15).

The concept of a quasi-steady state channel developed in a homogeneous soil due to a constant discharge is an oversimplification of processes occurring in natural channels. However, the model described here does seem to explain empirically derived width-discharge relationships (12, 14). Moreover, the derived width-discharge equations have a hydraulic basis.

Explicit Solution:

When a rectangular channel is in erodible material, Eqs. 25-27 do not apply because the width is no longer a constant. The result is that the continuity and Manning velocity equation cannot be solved explicitly. However, if an equation specifying the distribution of shear stress around the wetted perimeter is introduced, then the equations can be solved simultaneously provided the shear stress distribution is explicit in terms of the flow depth and the hydraulic radius is about equal to the depth.

If d_* is the normalized depth ($d_* = d/w_p = d/w$) and $F(d_*) = (d_*)/\bar{\tau}$ where w_p is wetted perimeter, τ is shear stress, and $\bar{\tau}$ is average shear stress for the cross-section, then $F(d_*)$ specifies the normalized distribution of shear stress along the wetted perimeter. As in the implicit solution, if we set this normalized shear stress equal to the normalized critical shear stress and solve for d_*, the result is the depth corresponding to the final eroded width. That is, let

$$F(d_*) = \frac{\tau_c}{\bar{\tau}} = \frac{\tau_c}{\gamma S d} \tag{39}$$

where τ_c is critical shear stress (lbs/ft^2), γ is specific weight (lbs/ft^3), and S is bed slope. Combining the continuity equation (Eq. 4) and the Manning equation (Eq. 9), the result is

$$Q = \frac{1.49}{n} S^{1/2} \, wd \, d^{2/3} \tag{40}$$

which can be rearranged as

$$w^{3/5} d = \left(\frac{1}{1.49}\right)^{3/5} S^{-3/10} \, n^{3/5} \, Q^{3/5}. \tag{41}$$

The procedure is to solve Eq. 39 for d and then substitute the solution for d into Eq. 41 and solve for the final eroded width w. Given the width-discharge equation, Eq. 41 can be solved for the depth, and Eq. 9 for the velocity. These solutions represent an explicit formulation for the hydraulic geometry.

The explicit procedure described above has been used together with several simple shear stress distributions (functions for $F(d_*)$) to obtain hydraulic geometry equations. However, no simple distributions of the form $F(d_*) = c d_*^p$ result in explicit forms of the derived hydraulic geometry that reproduce the observed relations between hydraulic geometry exponents at a station and downstream for a wide range of width-depth ratios. Therefore, additional research is required to specify the distribution of shear stress around the wetted perimeter of a channel cross-section (9, 7).

Instead of specifying the shear stress distribution, additional constraints on velocity, depth, width, and slope can be introduced (10) or assumptions made on the rate of change of water and sediment discharge in the downstream direction (18). Smith (18) assumed linear increases in water and sediment discharge in the downstream direction, and thus a constant sediment concentration, to derive the hydraulic geometry exponents. In view of changes in sediment transport capacity in the downstream direction (4) the assumption of constant concentration may be restrictive.

DISCUSSION AND SUMMARY

Discussion:

A brief sensitivity analysis was performed to assess the sensitivity of the implicit model (Eq. 34-36) to errors in the input parameters or changes in runoff rate. These data are summarized in Table 5. Column 2 of Table 5 shows which parameter was varied about the base or starting values by ±25 and ±50%. Columns 3 and 4 show the computed channel widths and the ratio of the computed widths to the width computed using the base values. Similar values for the total sediment yield from the developing rill are shown in columns 5 and 6. The values in column 6 are the same as the values in column 4 (except for computational errors from numerically integrating Eq. 35) because we assumed the same depth to the nonerodible boundary (d_{soil}) and the same total length of the rill (L = 15 ft) in each of the simulation runs. In this analysis, each parameter value was varied individually about its base value so that no parameter interactions were allowed. This is a simplification, because it is unlikely that the resistance (n), critical shear stress (τ_c), and slope (S) would be independent under real conditions. Nonetheless, the analysis shows model sensitivity to variations in the individual parameters.

Relative sensitivity of the implicit model is shown in Fig. 2. The final eroded channel width varies about as $Q^{1/2}$ but varies inversely with the critical shear stress. The computed depths of flow were approximately proportional to $S^{-.3}$, while the average shear stress ($\bar{\tau}$ = RS) was proportional to S. Therefore, the resulting final eroded width was approximately proportional to $S^{.26}$. As shown in Table 5, the final eroded width was proportional to $\tau_c^{-.53}$.

In the rill erosion study, sediment yield was directly proportional to final eroded width, and thus, sediment yield varied with $Q^{.51}$. Unfortunately, no downstream data were taken, so we cannot determine the

TABLE 5.—SUMMARY OF SENSITIVITY ANALYSIS FOR THE IMPLICIT MODEL. DATA FROM THE RILL EROSION STUDY (2)

Simulation number	Parameter and % variation		Final eroded width w_f (ft)	w_f/w_o	Sediment yield Q_s (lbs)	Q_s/Q_{so}	Comments
(1)	(2)		(3)	(4)	(5)	(6)	(7)
1	Base values		w_o = 0.596	1.00	Q_{so} = 89.1	1.00	Base value run:
2	-50	Q	.403[1]	.68	61.3	.69	Q = .0441
3	-25	Discharge	.507	.85	76.3	.86	n = .0347
4	+25		.676	1.13	100.6	1.13	τ_c = .110
5	+50		.749	1.26	111.1	1.25	S = .094
6	-50	n	.403	.68	61.3	.69	Symetric
7	-25	Resistance	.507	.85	76.3	.86	in n and Q
8	+25		.676	1.13	100.6	1.13	
9	+50		.749	1.26	111.9	1.25	
10	-50	τ_c	.839	1.41	123.5	1.39	
11	-25	Critical	.688	1.15	102.3	1.15	
12	+25	shear	.532	.89	79.9	.90	
13	+50	stress	.484	.81	72.9	.82	
14	-50	S	.497	.83	74.8	.84[2]	
15	-25	Slope	.558	.94	83.7	.94	
16	+25		.626	1.05	93.4	1.05	
17	+50		.651	1.09	97.0	1.09	

[1] Resulting width-discharge equation at a station is $w = 2.9\ Q^{.51}$.
[2] Shear stress increases with slope at a faster rate than the hydraulic radius decreases.

downstream hydraulic geometry or the downstream variation in sediment yield.

SUMMARY

To assess the response of stream channels to changing land use, it is necessary to express the relations between channel morphology and sediment yield.

Relations between hydrologic and hydraulic factors and channel geometry are referred to as hydraulic geometry. Analysis of hydraulic geometry for nonerodible channels suggested relationships between hydraulic geometry exponents at a station and downstream. Explicit expressions for hydraulic geometry in erodible channels can be derived by assuming a distribution for shear stress around the wetted perimeter. However, experimental determination of shear stress distributions is required to develop realistic hydraulic geometry.

A simplified, but implicit, model for channel morphology-sediment yield has been developed. The simple model reproduced observed sediment yield data and hydraulic geometry from an experimental rill study.

A brief sensitivity analysis was conducted to estimate channel response (final eroded width and sediment yield) in response to changing discharge, hydraulic resistance, critical shear stress, and channel slope.

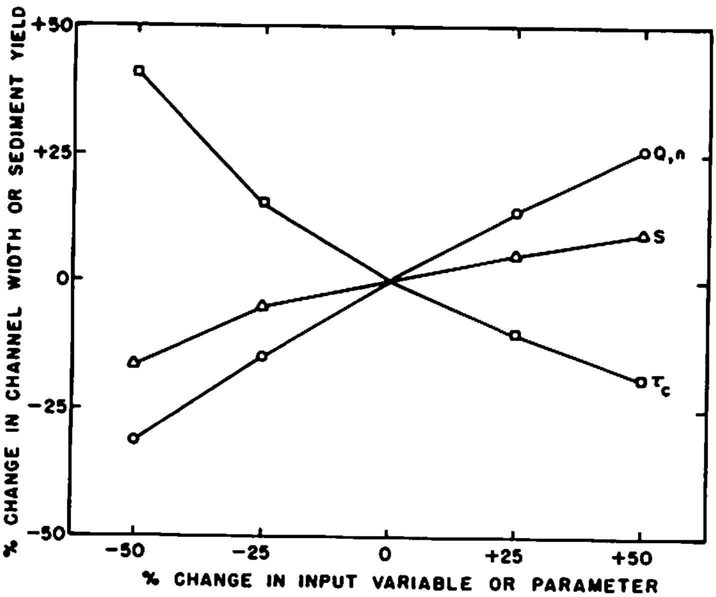

FIG. 2.—SENSITIVITY OF THE IMPLICIT CHANNEL MORPHOLOGY-SEDIMENT YIELD MODEL TO ERRORS IN INPUT. DATA FROM THE RILL EROSION STUDY (2)

If changes in land use are reflected in discharge, hydraulic resistance, critical shear stress, or channel slope, then the simplified, implicit model presented here can be used to assess the influence of such changes on sediment yield from small channels.

The USDA Soil Conservation Service has developed procedures to estimate runoff under various land uses (19). The influence of vegetation and tillage practices on Manning's resistance parameter has been tabulated (3). Basic relationships between soil characteristics and critical shear stress for agricultural soils have been investigated (17), and similar relationships from a variety of sources are summarized by Graf (4).

Our results showed that channel widths increase as discharge and hydraulic resistance increase and that narrower channels would result from a larger critical shear stress. Therefore, land use that causes these changes will cause a readjustment in streams. Changes in sediment yield -- for example, changes in the amount of sediment eroded from the channel boundary as the boundary adjusts to changing discharge -- will reflect the changes in land use. Previously, it was qualitatively known that streams make these adjustments. However, our analysis provides a basis, from known hydraulic relationships, to quantitatively evaluate the adjustments as they are influenced by a single variable such as discharge or by the interactions of discharge and slope, hydraulic resistance, or critical shear stress.

APPENDIX I.—REFERENCES

1. Barnes, H. H., "Roughness Characteristics of Natural Channels," U.S. Geological Survey Water Supply Paper 1849, 1967, 213 pp.
2. Foster, G. R., and Lane, L. J., "Simulation of Erosion and Sediment Yield from Field-Sized Areas," presented at the Conference on Water shed Management and Land Development in the Tropics, International Institute of Tropical Agriculture, Ibadan, Nigeria, Nov. 20-24, 1979, 29 pp.
3. Foster, G. R., Lane, L. J., and Nowlin, J. D., "A Model to Estimate Sediment Yield from Field-Sized Areas: Selection of Parameter Values." CREAMS - A Field Scale Model for Chemicals, Runoff, and Erosion from Agricultural Management Systems, Vol. II: User Manual, Washington, D.C., U.S. Dept. of Agriculture, Science and Education Administration. Manuscript in press, 1980.
4. Graf, W. H., Hydraulics of Sediment Transport. McGraw-Hill Book Co., New York, 1971, 513 pp.
5. Henderson, F. M., Open Channel Flow, Macmillan Co., New York, 1966, 522 pp.
6. Horton, R. E., "Erosional Development of Streams and their Drainage Basins: Hydrophysical Approach to Quantitative Morphology," Vol. 56, Bulletin Geological Society of America, 1945, pp. 273-370.
7. Kartha, V. C., and Leutheusser, H. J., "Distribution of Tractive Force in Open Channels," Proc. ASCE, Journal of the Hydraulics Division, Vol. 96(HY7), 1970, pp. 1469-1483.
8. Knighton, D. A., "Variation in Width-Discharge Relation and Some Implications for Hydraulic Geometry," Geological Society of America Bulletin, Vol. 85, 1974, pp. 1069-1076.
9. Lane, E. W., "Design of Stable Channels," Proceedings of the ASCE, Vol. 120, Separate No. 280, 1953, pp. 1234-1260.
10. Langbein, W. B., "Geometry of River Channels," Proceedings of the ASCE, Journal of the Hydraulics Division, Vol. 90(HY2), 1964, pp. 301-312.
11. Leopold, L. B., and Maddock, T. Jr., "The Hydraulic Geometry of Stream Channels and Some Physiographic Implications," U.S. Geological Survey Professional Paper 252, 1953.
12. Leopold, L. B., and Miller, J. P., "Ephemeral Streams-Hydraulic Factors and their Relation to the Drainage Net," U.S. Geological Survey Professional Paper 282-A, 1956, 32 pp.
13. Leopold, L. B., Wolman, M. G., and Miller, J. P., Fluvial Processes in Geomorphology, W. H. Freeman and Co., San Francisco, 1964, 522 pp.

14. Osterkamp, W. R., "Effect of Channel Sediment on Width-Discharge Relations, with Emphasis on Streams in Kansas," Bulletin No. 21, Kansas Water Resources Board, 1977, 25 pp.
15. Parker, R. S., "Experimental Study of Drainage Basin Evolution and Its Hydrologic Implications," CSU Hydrology Paper No. 90, Colorado State University, Fort Collins, Colorado, 1977, 58 pp.
16. Richards, K. S., "Hydraulic Geometry and Channel Roughness-A Non-Linear System," American Journal of Science, Vol. 273, 1973, pp. 877-896.
17. Smerdon, E. T., and Beasly, R. P., "The Tractive Force Theory Applied to Stability of Open Channels in Cohesive Soils," Univ. of Missouri, Agricultural Experiment Station Research Bulletin 715, 1959.
18. Smith, T. R., "A Derivation of the Hydraulic Geometry of Steady-State Channels from Conservation Principles and Sediment Laws," Journal of Geology, Vol. 82, 1974, pp. 98-104.
19. U.S. Department of Agriculture, Soil Conservation Service, National Enginering Handbook, Section 4, "Hydrology," 1972, 548 pp.
20. Wolman, M. G., "The Natural Channel of Brandywine Creek, Pennsylvania," U.S. Geological Survey Professional Paper 271, 1955, 56 pp.